

Harald Richter*

Bureau of Meteorology Training Centre, Melbourne, Australia

1. INTRODUCTION

Atmospheric vortices that commonly reach tornadic strength occur due to two different (but overlapping) processes. Non-supercell tornadoes, colloquially referred to as “landspouts” over land and “waterspouts” over water, are usually laminar and partially translucent or invisible vortices that are associated with rapidly growing towering cumulus and/or cumulonimbus clouds. They tend to occur in low-shear environments and draw their angular momentum from preexisting vertical vorticity supplied along a near-surface boundary or wind shift line. The growing updraft aloft stretches the vertical vorticity to create small-scale rotation that can reach tornadic wind speeds.

Supercell tornadoes utilize a second source of vertical vorticity – the tilting of horizontal vorticity inherent in strong vertical wind shear profiles. Supercell tornadoes are associated with a rotating parent storm (the supercell) and have the potential to be significantly stronger than their non-supercell counterparts.

During 04 August 2006 a tornado struck the Sydney suburb of La Perouse (Fig. 1). Based on this event, this paper has two goals: 1. to demonstrate that the storm environment was supportive of supercell tornadogenesis and therefore provided forecasters with an expectation of enhanced tornadic storm potential and 2. to identify the tornadic storm in the Kurnell radar base velocity and base reflectivity data.

2. THE STORM ENVIRONMENT FOR THE 04 AUGUST 2006 CASE



Fig. 1: The La Perouse tornado while crossing into Botany Bay (Courtesy of Channel 7, Australia)

The synoptic setup on the day was characterized by a surface high to the southwest (Fig. 2) and a cut-off cold pool at 500 hPa over the Sydney area (Fig. 3).

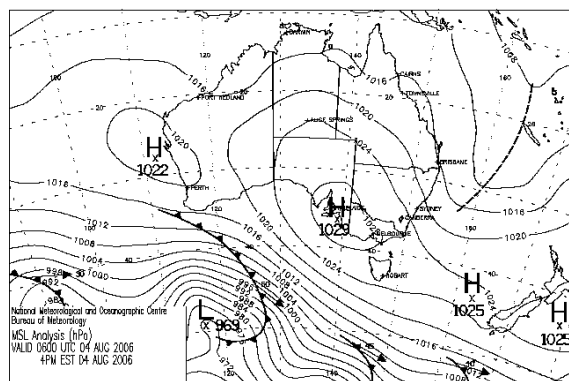


Fig. 2: 00z/04 surface analysis showing a northwest to southeast oriented surface pressure ridge west of the Sydney area and a surface trough reaching into the area from the northeast.

*Corresponding author address: Harald Richter,
Bureau of Meteorology Training Centre, PO Box
1289K, Melbourne VIC 3001, Australia; e-mail:
h.richter@bom.gov.au

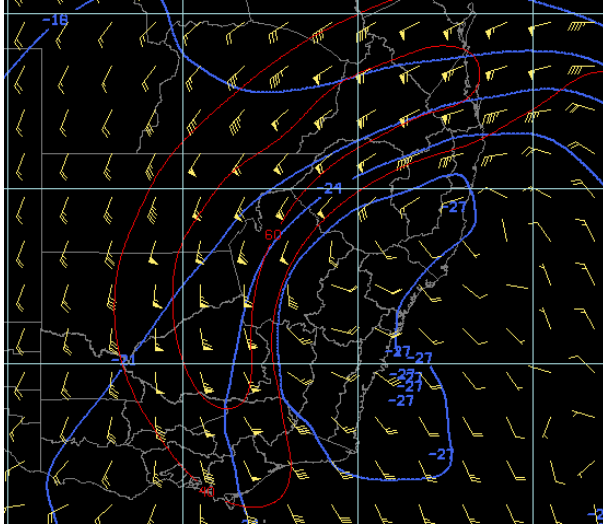


Fig. 3: Meso-LAPS 3h forecast of the temperature and wind field at 500 hPa valid at 03z/04 August 2006.

Fig. 3 shows a three-hour Meso-LAPS forecast of the wind and temperature fields at 500 hPa (Meso-LAPS is the Australian operational mesoscale numerical weather prediction model; Puri et al. 1998). A 60 kt jet is pivoting around the northwestern flank of the mid-level cold pool keeping the strongest deep layer shear in the region well inland.

The associated low-level shear profile and surface lifted index to 700 hPa is shown in Fig. 4. Modest

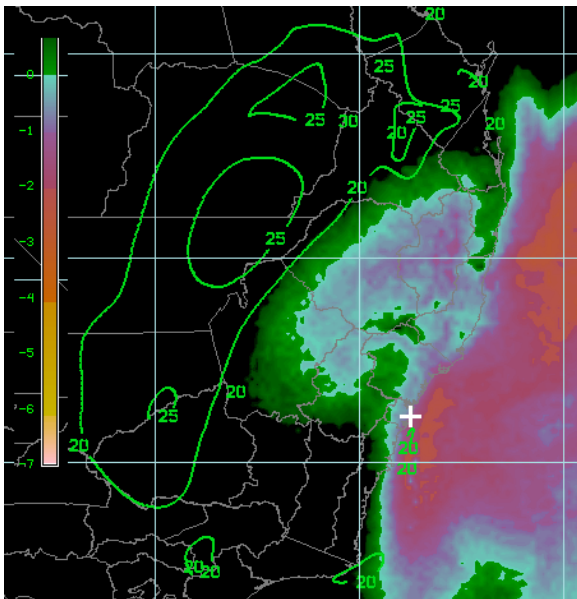


Fig. 4: Meso-LAPS surface lifted index at 700 hPa and low-level shear (maximum shear between model sigma level 0.9875 and the 1.5 km – 3 km layer) at 03z. The white “+” symbol marks the location of the tornado.

instability is apparent, driven primarily by the higher dewpoints over the sea. Most of the model’s low-level shear (see figure caption for details) is removed from the instability to the northwest, but the model provides a hint at ~20 kt shear values near the Sydney coast.

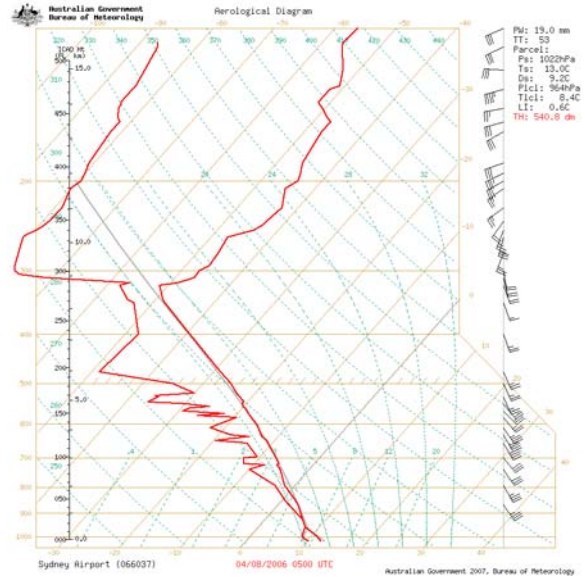


Fig. 5: 04z/04 Sydney airport sounding.

The 04z/04 Sydney sounding is shown in Fig. 5. A deep high relative humidity flow from the southeast is associated with a nearly moist adiabatic lapse rate from just above a shallow boundary layer up to the tropopause at just below 300 hPa.

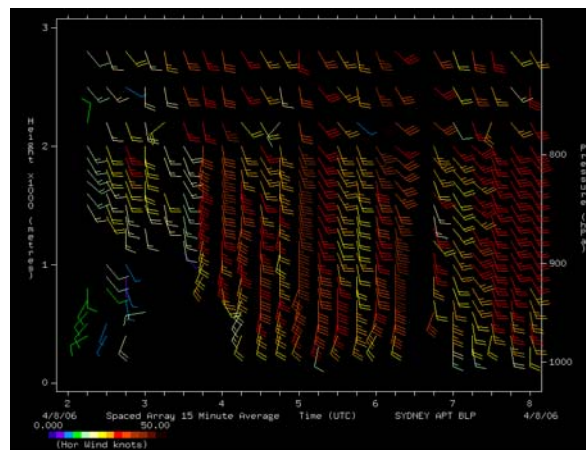


Fig. 6: Sydney airport profiler data around the time of the tornado occurrence.

The saturated air at low levels prevents the formation of overly cold downdrafts as shown by

the results from the VORTEX experiment in 1994-1995 (Rasmussen et al. 1994; Markowski et al. 2002).

A closer look at the 0615 UTC low-level shear profile from the Sydney airport wind profiler in Fig. 6 shows a 20 kt SSW flow just above the surface backing to a 40-45 kt S flow around 1 km. This equates to a 0-1 km bulk shear value of 35 kt. Measuring around 30 knots, the shear to approximately 3km ASL at 0615 UTC is less than the 0-1 km bulk shear, but should still support overall updraft rotation. The observed 0-1 km shear values far exceed the Meso-LAPS predicted low-level (approximately surface to 850 hPa) shear values in Fig. 4 indicating that the storm environmental focus needs to concentrate on a very shallow layer above the surface for cool season supercell tornadogenesis. Fig. 5 also shows that parcels with buoyancy values slightly larger than that of the boundary layer mean mixed parcel of the 04z sounding possess some low-level CAPE, a second ingredient thought to be vital in cool season tornadogenesis (Davies 1993; Davies 2006).

3. RADAR SIGNATURES OF THE TORNADIC STORM

Most supercell tornadogenesis studies focus on warm season cases over the U.S. Southern Great Plains (e.g., Wakimoto and Atkins 1996; Rasmussen et al. 2000). Fewer studies looked at “cold-core” tornadic supercells (Davies 2006), and even fewer studies exist on Australian cool season tornadoes (Hanstrum et al. 2002). This paucity of documented cool season Australian tornado cases was a first reason for the inception of this paper.

Secondly, the tornadic storm passed very close to the Kurnell Doppler radar located near the Sydney airport and therefore provides a rare opportunity to document cool season tornadic velocity signatures.

The Kurnell radar is a WF100-6C/12 radar with a beam width of 1° running in a staggered PRF mode (666 and 1000 Hz) to yield a Nyquist velocity of 26.6 ms⁻¹.

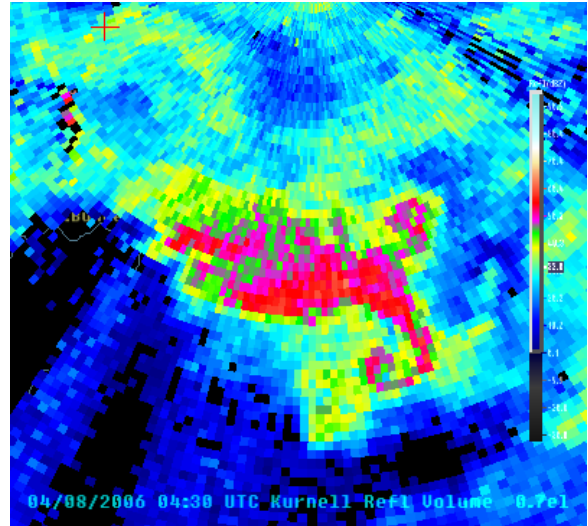


Fig. 7: Low-topped supercell at 0430z over the sea with the hook about 12 km SSE of the Kurnell radar.

One of the most remarkable radar signatures of the day occurred at 0430z, before the observed tornado. The reflectivity hook at ~200 m ASL (Fig. 7) is collocated with a circulation with a rotational velocity of 12.6 ms⁻¹ (see Fig. 8; rotational velocity determination carried out off unfiltered velocity data, not shown).

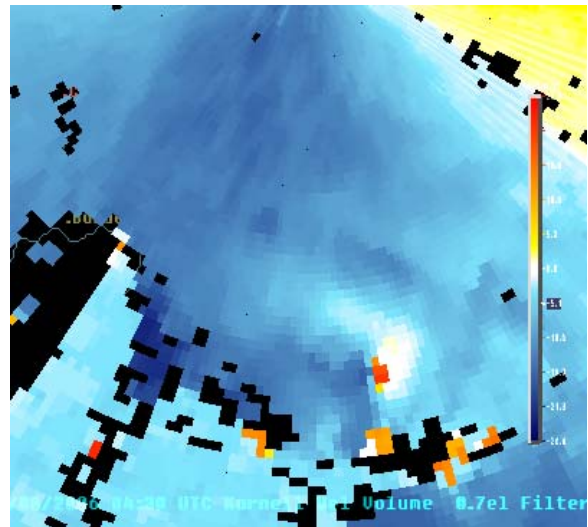


Fig. 8: The filtered velocity signature corresponding to Fig. 7.

Ironically, the time of the La Perouse tornado has not been reported thus far. However, only one Kurnell radar circulation signature matches the known location at “tornado landfall” near La Perouse (Figs. 9 and 10). At that time, the parent storm has a strung-out reflectivity appearance at low levels (around 1 km ASL).

The suspected tornadic circulation is embedded in the eastern end of the low-level core. At a height of ~600 m ASL the radar-measured rotational velocity is merely 9.1 ms^{-1} (Fig. 10). The velocity and reflectivity data from Kurnell over La Perouse are plotted in 250 m (range) x 70 m (azimuth) pixels and therefore should resolve at least part of the tornadic circulation near La Perouse, located 3.9 km to the NNE of the Kurnell radar. The couplet in Fig. 10 also shows good space-time continuity appearing in all tilts of the 0610z base scan while moving N with tilt elevation.

Video footage from the tornado showed a roof being “lifted off” a house indicating that the surface vortex almost certainly exceeded the damaging wind threshold around 50 knots. The apparent mismatch with the far weaker rotational velocity shown in Fig. 10 (~18 knots) suggests that either the tornadic winds were confined to a small area compared to radar sampling volume, or that tornadic circulation quickly lost intensity with height above the surface.

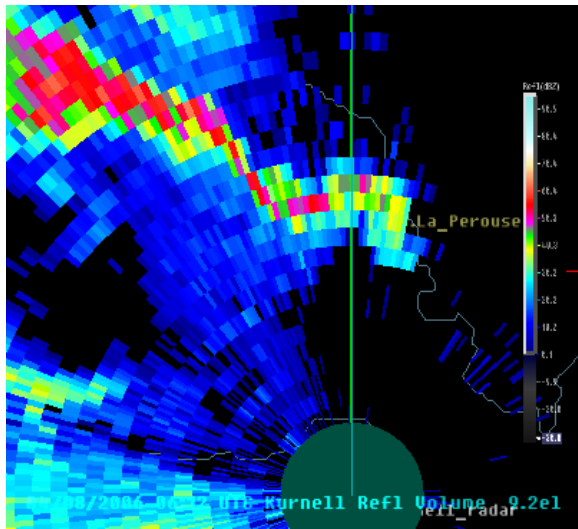


Fig. 9: Reflectivity signature during the assumed time of the La Perouse tornado.

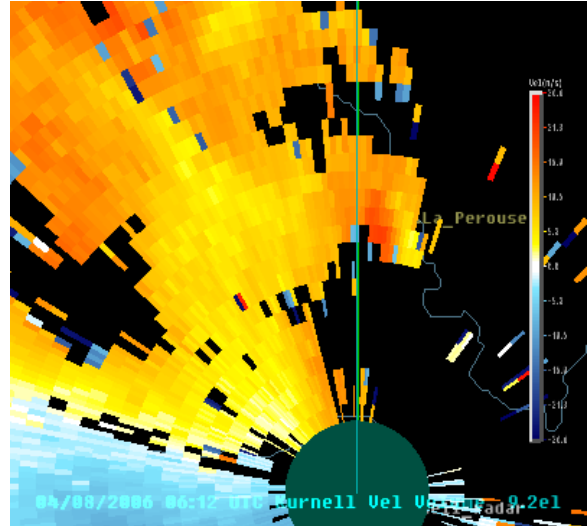


Fig. 10: The circulation signature corresponding to Fig.9 at the time when the radar-observed circulation was closest to La Perouse. The radar slices through the circulation at ~600 m ASL.

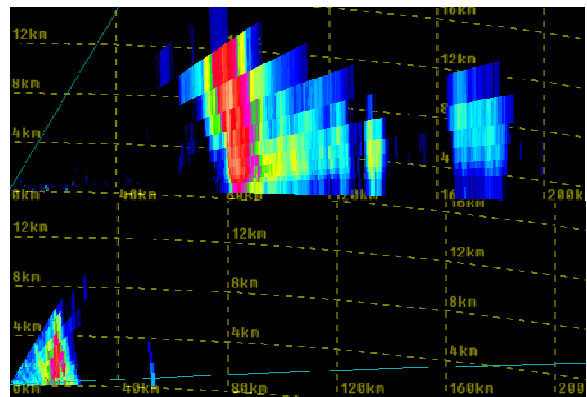


Fig. 11: Size comparison between a summertime Brisbane hailstorm (example taken from 08 November 2006) and a representative low-topped rotating storm on 04 August 2006.

A size comparison of the reflectivity cores of a representative core for the 04 August 2006 event and an equally representative core of a warm season hailstorm near Brisbane is shown in Fig. 11. This comparison highlights that more traditional radar reflectivity interrogation techniques (e.g., assessment of the 50 dBZ echo top) are of little value for low-topped supercells during the cool season where reflectivity signatures look, by and large, quite unremarkable.

4. SUMMARY

Although not obvious from the general synoptic setup and operational model predictions, the low-level dynamic and thermodynamic profiles of the storm environment around Sydney on the afternoon of 04 August 2007 are supportive of occasionally strong low-level storm rotation. A number of rotation-induced radar signatures have been observed during the passage of a number of convective storms that demonstrate the impact of the low level shear profile on storm morphology and behavior. A tornado has been filmed by a Channel 7 television crew during the day near La Perouse, a suburb of Sydney. Only one moderately weak rotational signature could be matched to the tornado report which arrived without a time of observation. The observed velocity couplets, despite high spatial resolution, show only weak rotation with rotational velocities in the 9-13 ms⁻¹ range. The reflectivity signatures, apart from curved core segments that appeared in some of the scans, are also unremarkable is significantly smaller in size than any warm season hail core signature. This demonstrates that cool season tornadic events, even when sampled close to a high resolution Doppler radar, are hard to diagnose in terms of their capacity to generate damaging surface winds.

REFERENCES

Davies, J. M., 1993: Small tornadic supercells in the central plains. Preprints, 17th Conf. Severe Local Storms, St. Louis, Missouri; pp. 305-309.

Davies, J. M., 2006: Tornadoes with cold core 500-mb Lows. *Wea. Forecasting*, **21**, pp. 1051-1062.

Hanstrum, B.N., G. A. Mills, A. Watson, J. P. Monteverdi and C. A. Doswell III, 2002: The cool-season tornadoes of California and Southern Australia. *Wea. Forecasting*, **17**, pp. 705-722.

Markowski, P. M., J. M. Straka and E. N. Rasmussen, 2002: Direct surface thermodynamic observations within the rear-flank downdrafts of nontornadic and tornadic supercells. *Mon. Wea. Rev.*, **130**, pp. 1692-1721.

Puri, K., G. S. Dietachmayer, G. A. Mills, N. E. Davidson, R. A. Bowen, and L. W. Logan, 1998: The new BMRC Limited Area Prediction System, LAPS. *Aust. Met. Mag.*, **47**, pp. 203-223.

Rasmussen, E. N., S. Richardson, J. M. Straka, P. M. Markowski and D. O. Blanchard, 2000: The association of significant tornadoes with a baroclinic boundary on 2 June 1995. *Mon. Wea. Rev.*, **128**, pp. 174-191.

Rasmussen, E.N., J. M. Straka, R. Davies-Jones, C. A. Doswell III, F. H. Carr, M. D. Eilts, and D. R. MacGorman, 1994: Verification of the Origins of Rotation in Tornadoes Experiment: VORTEX. *BAMS*, **75**, pp. 995-1006.

Wakimoto, R. M., and N. T. Atkins, 1996: Observations on the origins of rotation: The Newcastle tornado during VORTEX 94. *Mon. Wea. Review*, **124**, pp. 384-407.
